Large Anhydrous Polyalanine Ions: Evidence for Extended Helices and Onset of a More Compact State

Anne E. Counterman and David E. Clemmer*

Contribution from the Department of Chemistry, Indiana University, Bloomington, Indiana 47405

Received November 19, 1999

Abstract: Ion mobility measurements and molecular modeling calculations have been used to examine the conformations of large multiply charged polyalanine peptides. Two series of $[Ala_n+3H]^{3+}$ conformations which do not interconvert during the 10 to 30 ms experimental timescales are observed: a family of elongated structures for $n = 18$ to 39 and a series of more compact conformations for $n = 24$ to 41. The more compact state becomes the dominant conformer type for $n > 32$. Molecular modeling studies and comparisons of calculated collision cross sections with experiment indicate that the elongated ions have extended helical conformations. We suggest that the more compact state corresponds to a new conformer type: a folded hinged helix-coil state in which helical and coil regions have similar physical dimensions. The competition between extended and compact states is rationalized by considering differences in charge stabilization and entropy.

Introduction

Polypeptide chains with fewer than ~30 residues rarely exhibit defined tertiary structures in solution unless stabilized by disulfide bonds or metal cations.[1] An exception is a 23 residue sequence that has been engineered to fold into a well-defined β-hairpin-α-helix structure by an iterative design process.[2] An understanding of the intrinsic properties of peptides that stabilize a first fold is key to *de novo* synthesis of specific motifs. Recently several groups have investigated the structures of peptide ions in the gas phase, where conformations can be established in the complete absence of solvent.[3−12] These studies provide direct information about the role of intramolecular interactions in determining biomolecular structure.

Alanine-based polymers provide a natural target for gas-phase studies because of the extensive experimental work on these systems in solution and the solid phase and more recent studies of gas-phase ions. Early crystal structures showed that alanine had the highest propensity of any naturally occurring amino acid to be found in regions of helices.[13−15] A debate in the literature as to whether the alanine residue is intrinsically stabilizing in solution is ongoing.[16−18] Additionally, several groups have used alanine polymers doped with other residue types (Lys, Ile, Leu, Phe, and Val) to explore factors that disrupt helix stability in solution.[19] Hudgins et al.[20] and Samuelson et

(1) DeGrado, W. F.; Summa, C. M. *Annu. Rev. Biochem.* **1999**, *68*, 779.
(2) Struthers, M. D.; Cheng, R. P.; Imperiali, B. *Science* **1996**, *271*, 342.
(3) (a) Covey, T. R.; Douglas, D. J. *J. Am. Soc. Mass Spectrom.* **1993**, *4*, 616. (b) Cox, K. A.; Julian, R. K.; Cooks, R. G.; Kaiser, R. E. *J. Am. Soc. Mass Spectrom.* **1994**, *5*, 127. (c) Collings, B. A.; Douglas, D. J. *J. Am. Chem. Soc.* **1996**, *118*, 4488. (d) Chen, Y.-L.; Collings, B. A.; Douglas, D. J. *J. Am. Soc. Mass Spectrom.* **1997**, *8*, 681.
(4) (a) von Helden, G.; Wyttenbach, T.; Bowers, M. T. *Science* **1995**, *267*, 1483. (b) Wyttenbach, T.; von Helden, G.; Bowers, M. T. *J. Am. Chem. Soc.* **1996**, *118*, 8355.
(5) (a) Clemmer, D. E.; Hudgins, R. R.; Jarrold, M. F. *J. Am. Chem.* Soc. **1995**, *117*, 10141. (b) Shelimov, K. B.; Clemmer, D. E.; Hudgins, R. R.; Jarrold, M. F. *J. Am. Chem. Soc.* **1997**, *119*, 2240. (c) Shelimov, K. B.; Jarrold, M. F. *J. Am. Chem. Soc.* **1997**, *119*, 9586.
(6) (a) Valentine, S. J.; Clemmer, D. E. *J. Am. Chem. Soc.* **1997**, *119*, 3558. (b) Valentine, S. J.; Anderson, J.; Ellington, A. E.; Clemmer, D. E. *J. Phys. Chem. B* **1997**, *101*, 3891. (c) Valentine, S. J.; Counterman, A. E.; Clemmer, D. E. *J. Am. Soc. Mass Spectrom.* **1997**, *8*, 954.
(7) (a) Winter, B. E.; Light-Wahl, K. J.; Rockwood, A. L.; Smith, R. D. *J. Am. Chem. Soc.* **1992**, *114*, 5897. (b) Suckau, D.; Shi, Y.; Beu, S. C.; Senko, M. W.; Quinn, J. P.; Wampler, F. M.; McLafferty, F. W. *Proc. Natl. Acad. Sci. U.S.A.* **1993**, *90*, 790. (c) Wood, T. D.; Chorush, R. A.; Wampler, F. M.; Little, D. P.; O'Connor, P. B.; McLafferty, F. W. *Proc. Natl. Acad. Sci. U.S.A.* **1995**, *92*, 2451. (d) Cassady, C. J.; Carr, S. R. *J. Mass Spectrom.* **1996**, *93*, 3143.
(8) (a) Ogorzalek Loo, R. R.; Smith, R. D. *J. Am. Soc. Mass Spectrom.* **1994**, *5*, 207. (b) Ogorzalek Loo, R. R.; Winger, B. E.; Smith, R. D. *J. Am. Soc. Mass Spectrom.* **1994**, *5*, 1064. (c) Schnier, P. F.; Gross, D. S.; Williams, E. R. *J. Am. Chem. Soc.* **1995**, *117*, 6747. (d) Williams, E. R. *J. Mass Spectrom.* **1996**, *31*, 831. (e) Rodriguez-Cruz, S. E.; Klassen, J. S.; Williams, E. R. *J. Am. Soc. Mass Spectrom.* **1997**, *8*, 565. (f) Zhang, X.; Cassady, C. J. *J. Am. Soc. Mass Spectrom.* **1996**, *7*, 1211. (g) Sterner, J. L.; Johnston, M. V.; Nicol, G. R.; Ridge, D. P. *J. Am. Soc. Mass Spectrom.* **1999**, *10*, 483.
(9) (a) Kaltashov, I. A.; Fenselau, C. C. *J. Am. Chem. Soc.* **1995**, *117*, 9906. (b) Adams, J.; Strobel, F.; Reiter, A. *J. Am. Soc. Mass Spectrom.* **1996**, *7*, 30. (c) Kaltashov, I. A.; Fenselau, C. C. *Proteins* **1997**, *27*, 165.
(10) Fye, J. L.; Woenckhaus, J.; Jarrold, M. F. *J. Am. Chem. Soc.* **1998**, *120*, 1327.
(11) McLuckey, S. A.; Goeringer, D. E. *Anal. Chem.* **1995**, *67*, 2493. Stephenson, J. L., Jr.; McLuckey, S. A. *J. Am. Chem. Soc.* **1996**, *118*, 7390. Stephenson, J. L., Jr.; McLuckey, S. A. *Anal. Chem.* **1996**, *68*, 4026. McLuckey, S. A.; Stephenson, J. L., Jr.; Asano, K. G. *Anal. Chem.* **1998**, *70*, 1198. Stephenson, J. L., Jr.; McLuckey, S. A. *J. Am. Soc. Mass Spectrom.* **1998**, *9*, 585.
(12) Sullivan, P. A.; Axelsson, J.; Altmann, S.; Quist, A. P.; Sunqvist, B. U. R.; Reimann, C. T. *J. Am. Soc. Mass Spectrom.* **1996**, *7*, 329. Reimann, C. T.; Sullivan, P. A.; Axelsson, J.; Quist, A. P.; Altmann, S.; Roepstorff, P.; Velazquez, I.; Tapia, O. *J. Am. Chem. Soc.* **1998**, *120*, 7608.
(13) Chou, P. Y.; Fasman, G. D. *Biochemistry* **1974**, *13*, 222.
(14) O'Neil, K. T.; DeGrado, W. F. *Science* **1990**, *250*, 646.
(15) Chakrabartty, A.; Baldwin, R. L. *Adv. Protein Chem.* **1995**, *46*, 141.
(16) Ingwall, R. T.; Scheraga, H. A.; Lotan, N.; Berger, A.; Katchalski, E. *Biopolymers* **1968**, *6*, 331. Vila, J.; Williams, R. L.; Grant, J. A.; Wojcik, J.; Scheraga, H. A. *Proc. Natl. Acad. Sci. U.S.A.* **1992**, *89*, 7821.
(17) Kemp, D. S.; Boyd, J. G.; Muendel, C. C. *Nature* **1991**, *352*, 451. Renold, P.; Tsang, K. Y.; Shimizu, L. S.; Kemp, D. S. *J. Am. Chem. Soc.* **1996**, *118*, 12234. Groebke, K.; Renold, P.; Tsang, K. Y.; Allen, T. J.; McClure, K. F.; Kemp, D. S. *Proc. Natl. Acad. Sci. U.S.A.* **1996**, *93*, 4025.
(18) Spek, E. J.; Olson, C. A.; Shi, Z.; Kallenbach, N. R. *J. Am. Chem. Soc.* **1999**, *121*, 5571.
(19) See, for example: Padmanabhan, S.; Marqusee, S.; Ridgeway, T.; Laue, T. M.; Baldwin, R. L. *Nature* **1990**, *344*, 268. Millhauser, G. L.; Stenland, C. J.; Hanson, P.; Bolin, K. A.; van de Ven, F. J. M. *J. Mol. Biol.* **1997**, *267*, 963 and references therein.
(20) Hudgins, R. R.; Mao, Y.; Ratner, M. A.; Jarrold, M. F. *Biophys. J.* **1999**, *76*, 1591.

10.1021/ja9940625 CCC: $20.00
Published on Web 01/24/2001

al.[21] have shown that gas-phase polyalanine ions ($[Ala_n+H]^+$, $n = 3$ to 20) form nonspecific globular structures. In this system, the protonated amino terminus is solvated through multiple interactions with electronegative carbonyl backbone groups. Incorporation of a single Lys residue as the charge carrier at the C-terminus (i.e., $[Ala_n-Lys+H]^+$, $n = 5$ to 19) leads to a stable elongated helix; the butylammonium side chain can be capped by carbonyl groups without disrupting the $i \rightarrow i + 4$ hydrogen bond network.[22,23]

In this paper, we report ion mobility measurements[24,25] for a series of $[Ala_n+zH]^{z+}$ ions ($n = 5$ to 49; $z = 1$ to 4). We have focused primarily on the $[Ala_n+3H]^{3+}$ ions ($n = 18$ to 41), which exhibit two stable conformer families. The results indicate that the $[Ala_n+3H]^{3+}$ ions exist as an extended helical state (observed for $n = 18$ to 39) and a substantially more compact state that arises for polymers with 24 or more residues. Molecular modeling studies suggest that the compact state contains a helical C-terminal region, which is stabilized by interactions with protons on the N-terminal side of the polymer chain, which appears to have largely random structure. As the peptide length increases, the folded state competes effectively with the extended helical state, and becomes the dominant conformer for peptides with more than 32 residues. Charge location and entropic effects appear to be important in determining the onset of the first-folded state. Studies of the onset of folds in isolated peptides should complement efforts to understand folding in condensed media.[1,2]

Experimental Section

Ion Mobility/Time-of-Flight Measurements. Ion mobility/time-of-flight methods for analyzing peptide mixtures have been described previously;[25,26] only a brief description is given here. Solutions of polyalanine (Sigma, nominal 1000−5000 mol wt range; 5.6×10^{-5} to 2.8×10^{-4} M in a 49:49:2 water:acetonitrile:acetic acid mixture) were electrosprayed[27] at atmospheric pressure into a differentially pumped desolvation region and ions are introduced into the drift region through an ion channel.[28] Pulses (300 μs in duration) of ions were introduced into the drift region with use of an electrostatic ion shutter. The ions drift 58.23 cm through ~160 Torr of He buffer gas under the influence of a uniform 137.4 V·cm^{-1} field. The mobilities of the polypeptide ions through the gas under the influence of a weak uniform electric field depend on the polypeptide shapes and charge states. For a given charge state, compact geometries with relatively small collision cross sections have higher mobilities than more elongated structures.[29] A small fraction of the ions exit the drift region into a high-vacuum region ($\sim 5 \times 10^{-5}$ Torr) and are focused into the source region of an orthogonal time-of-flight mass spectrometer having a reflectron geometry. Here, high-voltage high-repetition pulses, synchronous with the initial drift gate pulses, are used to initiate *m*/*z* measurements. Because flight times in the mass spectrometer are much shorter than drift times in the drift tube, it is possible to record hundreds of flight-time distributions for each pulse of ions that is gated into the drift tube. Data were acquired by using a nested acquisition system that was developed in-house and described previously.[26]

Experimental Collision Cross Sections. The measured arrival times include the time required for ions to travel through drift gas as well as other regions of the instrument. To determine cross sections, it is necessary to correct the arrival times by the time ions spend in other regions of the instrument. These corrections are small (80 to 140 μs) relative to the 10 to 30 ms drift times. Experimental collision cross sections are derived from the corrected arrival times by the following relation[25]

$$\Omega = \frac{(18\pi)^{1/2}}{16}\frac{ze}{(k_b T)^{1/2}}\left[\frac{1}{m_I}+\frac{1}{m_B}\right]^{1/2}\frac{t_D E}{L}\frac{760}{P}\frac{T}{273.2}\frac{1}{N} \qquad (1)$$

where t_D is the drift time (determined from the maximum of each peak), E is the drift field; T and P are the temperature and pressure of the buffer gas, respectively; L is the drift tube length; ze is the ion's charge; N is the neutral number density; k_b is Boltzmann's constant; and m_I and m_B are the masses of the ion and buffer gas, respectively. The parameters E, L, P, T, and t_D can be precisely measured. The reproducibility of measured cross sections is excellent; the percent relative uncertainty of any two measurements is typically less than ±1.0%. Measurements were performed at low E/N such that mobilities are independent of the applied drift field and drift velocities are small compared with the thermal velocity of the buffer gas. Under these conditions, ions are not expected to align in the drift tube and we assume that collision cross sections correspond to an average of all possible orientations.

To emphasize structural differences between conformer families, we have defined an *effective asphericity* scale using the following relation:

$$\Omega_{asp} = \frac{\Omega - \Omega_{sphere}}{\Omega_{linear} - \Omega_{sphere}} \qquad (2)$$

where Ω_{sphere} and Ω_{linear} are the cross sections expected for globular and extended linear ions having the molecular weight of the ion of interest, respectively.[30] On this relative scale, compact $[Ala_n+H]^+$ globules are assumed to be spherical, having $\Omega_{asp} \equiv 0.0$, and completely extended conformers have $\Omega_{asp} \equiv 1.0$.

Molecular Modeling Simulations and Cross Section/Asphericity Calculations. Model conformers for the $[Ala_n+2H]^{2+}$ and $[Ala_n+3H]^{3+}$ ions described here were generated with the InsightII molecular modeling software[31] using the Extensible Systematic force field (ESFF) and a dielectric of 1.0. Molecular dynamics simulations were carried out at 300 K for at least 0.25 ns. Many trajectories were allowed to run for up to 1.0 ns; no significant differences were observed between the distributions of conformers obtained from trajectories performed for 0.25 or 1.0 ns. Several initial starting structures [such as perfect $i \rightarrow i + 4$ (α-) and $i \rightarrow i + 3$ (3_{10}-) helices, linear geometries and random globules] were considered. In many cases, we have performed simulated annealing studies to generate conformations. The protocol used for these studies is similar to those described previously.[4b,32,33]

An important consideration in multiply charged ions is the initial charge site assignment. Williams[34] and Jarrold[35] have previously commented on the factorial nature of charge-site assignment, which leads to a large number of possible assignments. For example, there

(21) Samuelson, S.; Martyna, G. J. *J. Phys. Chem. B* **1999**, *103*, 1752.
(22) Hudgins, R. R.; Ratner, M. A.; Jarrold, M. F. *J. Am. Chem. Soc.* **1998**, *120*, 12974.
(23) Hudgins, R. R.; Jarrold, M. F. *J. Am. Chem. Soc.* **1999**, *121*, 3494.
(24) Hagen, D. F. *Anal. Chem.* **1979**, *51*, 870. Hill, H. H.; Siems, W. F.; St. Louis, R. H.; McMinn, D. G. *Anal. Chem.* **1990**, *62*, 1201A.
(25) For recent reviews of ion mobility studies of biomolecules see: Clemmer, D. E.; Jarrold, M. F. *J. Mass Spectrom.* **1997**, *32*, 577. Hoaglund Hyzer, C. S.; Counterman, A. E.; Clemmer, D. E. *Chem. Rev.* **1999**, *99*, 3037.
(26) Hoaglund, C. S.; Valentine, S. J.; Sporleder, C. R.; Reilly, J. P; Clemmer, D. E. *Anal. Chem.* **1998**, *70*, 2236. Henderson, S. C.; Valentine, S. J.; Counterman, A. E.; Clemmer, D. E. *Anal. Chem.* **1999**, *71*, 291.
(27) Fenn, J. B.; Mann, M.; Meng, C. K.; Wong, S. F.; Whitehouse, C. M. *Science* **1989**, *246*, 64.
(28) Li, J.; Taraszka, J. A.; Counterman, A. E.; Clemmer, D. E. *Int. J. Mass Spectrom. Ion Proc.* **1999**, *185*/*186*/*187*, 37.
(29) von Helden, G.; Hsu, M.-T.; Kemper, P. R.; Bowers, M. T. *J. Chem. Phys.* **1991**, *95*, 3835. Jarrold, M. F.; Constant, V. A. *Phys. Rev. Lett.* **1991**, *67*, 2994. Clemmer, D. E.; Hudgins, R. R.; Jarrold, M. F. *J. Am. Chem.* Soc. **1995**, *117*, 10141.
(30) Here, $\Omega_{sphere} = (-9.49 \times 10^{-4})n^3 + -0.213n^2 + 16.2n + 38.1$, as determined from a fit to experimental cross sections for globular $[Ala_n+H]^+$ ions; and $\Omega_{linear} = 25.95n + 27.75$, as determined from a fit to calculated cross sections (as described in ref 40) for linear structures.
(31) InsightII, Biosym/MSI: San Diego, CA, 1995.
(32) Hoaglund, C. S.; Liu, Y.; Pagel, M.; Ellington, A. D.; Clemmer, D. E. *J. Am. Chem. Soc.* **1997**, *119*, 9051.
(33) Counterman, A. E.; Clemmer, D. E. *J. Am. Chem. Soc.* **1999**, *121*, 4031.
(34) Williams, E. R. *J. Mass Spectrom.* **1996**, *31*, 831.
(35) Mao, Y.; Woenckhaus, J.; Kolafa, J.; Ratner, M. A.; Jarrold, M. F. *J. Am. Chem. Soc.* **1999**, *121*, 2712.

are 7140 [36!/(3! × (36 − 3)!)] possible charge site assignments for three charges placed on a polyalanine string with 36 protonatable sites. At least 10 charge site assignments (chosen to sample widely different structures) for each starting structure were considered for each of the polymer sizes that we have simulated. Protonation sites were assumed to be fixed at the N-terminus or −NH groups on the polymer backbone, and are denoted using values $i = 1$ to n from the N- to C-terminal residues, respectively.[36,37]

Cross sections for trial conformers were calculated by using the exact hard spheres scattering method (EHSS)[38] and the resulting values were normalized to those expected from the more rigorous trajectory calculation[39] by comparing cross sections for polyalanine globules and helices calculated by the EHSS method to values from trajectory calculations reported previously.[20,22] This approach is analogous to the method we used previously for deducing residue volumes.[41] The calibration used here[40] differs slightly from that used in previous studies[41] because the present systems are larger and less dense than those previously modeled. Values (reported as asphericities) are an average of the final 30 structures from each molecular dynamics simulation; in all cases, the final conformations that are observed appear to be representative structures of a distribution of low-lying accessible states (i.e., calculations performed for longer time periods, which were performed as a crosscheck of the modeling protocol, yield similar distributions of conformations).

Although multiple structures could have identical mobilities, structural assignments can become very reliable when structural families (as a function of size) exist.[22,42,43] In this case, the fit of calculated mobilities for different geometries as a function of size is substantially more selective for different structures. That is, it is much less likely that different conformer types have identical cross sections for all polymer sizes. An additional constraint is the calculated energies of different structures. When a model conformer type that agrees with experiment over a range of sizes is also the lowest energy structure found from simulations, rigorous assignments of structural motifs can be made.[22] The structural families that are observed for the polyalanine system and energies from molecular modeling simulations allow detailed insight into the structure of these systems.

Relative Energies of Final Model Structures and Structural Isomers. To gain a feeling for the relative stabilities of different conformer types, we have compared relative energies obtained from the modeling simulations. Rigorously, it is only valid to compare energies for conformers in which all covalent bonds are the same; that is, the number of bonds and atom hybridizations must be identical. This will be the case for all simulations where all three protons are placed on amide groups along the polypeptide backbone. In some cases, we have compared energies for conformers having a single proton placed at the N-terminus (i.e, the $i = 1$ position) and two additional protons placed along the backbone to energies calculated for conformers that are protonated solely on other backbone sites (i.e., all three protons are located at $i = 2$ or greater). In these comparisons, the nitrogen atom hybridizations differ. Comparison of simulations for six closely related charge assignments (e.g., protonation configurations such as 1, 19, 36 and 2, 19, 36) of $[Ala_{36}+3H]^{3+}$ shows that the relative energies for conformations protonated on the N-terminus are 3 to 8 kcal mol^{-1} lower than the values that are calculated for the corresponding backbone-only configuration. The calculated energies derived from simulations do not account for the difference in proton affinity of backbone sites with respect to the more basic N-terminus;[37] we estimate that a correction of ∼10 kcal·mol^{-1} should be added for charge configurations in which none of the protons are placed on the more basic amino terminus. Overall, the magnitude of the differences in energy between related charge site configurations is substantially smaller than energetic differences associated with very different conformations. In the discussions given below, we compare the lowest energy conformations that are found. Energies are reported as calculated; any corrections are specifically noted.

Results and Discussion

Ion Mobility/Time-of-Flight Measurements. Figure 1 shows a two-dimensional plot of a region of nested drift (flight) time data recorded for the mixture of polyalanine ions. Mass-to-charge ratios determined from flight times indicate that four charge states (which fall into families according to their mobilities) are present for different polyalanine chain lengths. Singly protonated $[Ala_n+H]^+$ ions are observed for small oligomers ($n = 5$ to 18); measured cross sections for these ions (eq 1) agree with the experimental $[Ala_n+H]^+$ results and globular structural assignments made previously.[20,21] Distributions of higher charge states $[Ala_n+2H]^{2+}$ ($n = 9$ to 29), $[Ala_n+3H]^{3+}$ ($n = 18$ to 41), and $[Ala_n+4H]^{4+}$ ($n = 29$ to 49) are also observed.[44] For example, the peaks at flight times of 29.68, 29.74, and 30.02 μs (at m/z values of 718.0, 721.0, and 734.4) are assigned to $[Ala_{30}+3H]^{3+}$, $[Ala_{20}+2H]^{2+}$, and $[Ala_{41}+4H]^{4+}$, respectively.

It is particularly interesting that many of the $[Ala_n+3H]^{3+}$ sizes exhibit two ion mobility peaks. Slices across the two-dimensional dataset at m/z values corresponding to $[Ala_n+3H]^{3+}$ ($n = 27$, 30, 33, and 34) are also shown in Figure 1. The two resolved peaks indicate that two stable families of conformations, which do not interconvert during the experimental timescales, must be present. The lower mobility (larger collision cross section) family is the only state observed for the small $[Ala_{18}+3H]^{3+}$ to $[Ala_{23}+3H]^{3+}$ sizes, and persists to $[Ala_{39}+3H]^{3+}$. The abundance of higher mobility (more compact) conformers increases with peptide length; for peptides with 32 or more residues (Figure 1), higher mobility ions are more abundant than the lower mobility species. Analysis of multiple data sets recorded under different solution and ion mobility conditions indicates that the compact conformers are always discernible at $n = 24$.

Figure 2 shows a plot of effective asphericities for all ions observed experimentally. The asphericities fall into conformer families for the +1 to +4 charge states, varying in asphericity from 0.0 to ∼0.5. Comparisons of the experimental Ω_{asp} values for the lower mobility family observed for $[Ala_{18}+3H]^{3+}$ to $[Ala_{39}+3H]^{3+}$ ions with values for Ω_{asp}($[Ala_n-Lys+H]^+$ helix)[22] and Ω_{asp}(model helix) suggest that these ions have extended structures with large α-helical regions. Shorter peptides

(36) Overall, the dominant force in the multiply charged polymers is Coulombic repulsion; the survey of charge site configurations performed here is intended to give a general look at the conformational behavior of these polymers, rather than details of charge site interactions. It has been suggested that backbone −C═O groups are more basic than backbone −NH groups [ref 37]; these were not included for consideration due to limitations of the available force fields. Because the high electronegativity of backbone carbonyl groups engages them in hydrogen bonding interactions with the protonation site, it is unlikely that the formal placement of the proton on the −NH portion of the backbone will significantly influence the molecular modeling results. Additionally, in the helical structures, protonation of any of the three carbonyls nearest the C-terminus (i.e., $i = n - 1$, $n - 2$, or $n - 3$; logical choices in terms of minimizing coulomb repulsion) would destabilize the final helical turn because of the absence of $i \rightarrow i + 4$ hydrogen bonding partners.

(37) Zhang, K.; Cassady, C. J.; Chung-Phillips, A. *J. Am. Chem. Soc.* **1994**, *116*, 11512.

(38) Shvartsburg, A. A.; Jarrold, M. F. *Chem. Phys. Lett.* **1996**, *261*, 86.

(39) Mesleh, M. F.; Hunter, J. M.; Shvartsburg, A. A.; Schatz, G. C.; Jarrold, M. F. *J. Phys. Chem.* **1996**, *100*, 16082.

(40) Cross sections have been calibrated according to the following relation: $\Omega_{EHSS}(cal) = -2.99 + 0.900\Omega_{EHSS} + (3.166 \times 10^{-5})\Omega_{EHSS}^2$. Over the critical size range discussed here, $n = 24$ to 40, we expect the calibrated EHSS cross sections to be accurate to within a few percent.

(41) Counterman, A. E.; Clemmer, D. E. *J. Am. Chem. Soc.* **1999**, *121*, 4031.

(42) von Helden, G.; Hsu, M. T.; Gotts, N.; Bowers, M. T. *J. Phys. Chem.* **1993**, *97*, 8182.

(43) Ho, K.-M.; Shvartsburg, A. A.; Pan, B. C.; Lu, Z. Y.; Wang, C. Z.; Wacker, J. G.; Fye, J. L.; Jarrold, M. F. *Nature* **1998**, *392*, 582.

(44) We rule out the possibility that multiply charged families are due to multimers based on the measured m/z ratios (e.g., m/z $[Ala_{10} + H]_2^{2+}$ =730.0 while m/z $[Ala_{20} + 2H]^{2+}$ = 721.0).

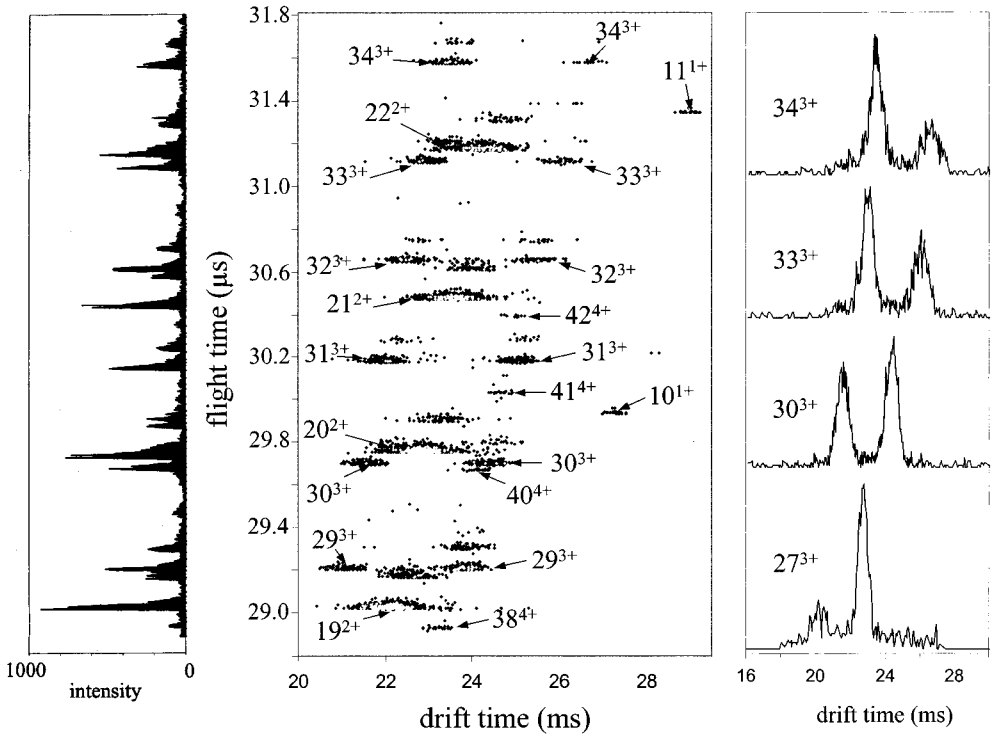

Figure 1. A region of nested drift (flight) times for an electrosprayed polyalanine mixture recorded with a buffer gas pressure of 163.5 Torr and an electric field strength of 137.4 V·cm^{-1}. The mass spectrum shown on the left is the sum of intensities at each flight time. Drift time distributions for $[Ala_{27}+3H]^{3+}$, $[Ala_{30}+3H]^{3+}$, $[Ala_{33}+3H]^{3+}$, and $[Ala_{34}+3H]^{3+}$ ions (obtained by taking slices of the two-dimensional data set) are shown on the right.

in this family, $[Ala_{18}+3H]^{3+}$ to $[Ala_{21}+3H]^{3+}$, appear to be more aspherical than α-helices. Presumably, the high coulomb energy associated with these short $[Ala_n+3H]^{3+}$ ions stretches them out. Asphericities for the higher mobility $[Ala_{24}+3H]^{3+}$ to $[Ala_{41}+3H]^{3+}$ peptides, and all of the $[Ala_n+2H]^{2+}$ peptides, fall between values that are expected for extended helical and compact globular $[Ala_n+H]^+$ conformations; these families must correspond to peptides that are at least partially folded.

Molecular Modeling Simulations of $[Ala_n+H]^+$ and $[Ala_n+2H]^{2+}$ Ions. To obtain further insight into the structures of these ions, we have employed molecular modeling techniques. Simulations of $[Ala_n+H]^+$ ($n = 8$, 12, 16) are in good agreement with results published previously by Hudgins et al.[20] and Samuelson et al.[21] These ions favor compact globular (largely random) structures; a distribution of electronegative backbone carbonyl groups solvate the protonated amino terminus. Such structures can be found from a variety of initial starting conditions including $i \rightarrow i + 3$ and $i \rightarrow i + 4$ helices, as well as linear and globular starting structures.

Simulations for several sizes of the $[Ala_n+2H]^{2+}$ peptides (n = 18, 24, and 28) yield structures that are similar to the $[Ala_n+H]^+$ globules;[20,21] regardless of the charge site configuration or initial structure, numerous related collapsed (globular) conformations in which charged sites are solvated by electronegative carbonyl groups are generated. Figure 3 shows several examples of low-energy conformers obtained for $[Ala_{18}+2H]^{2+}$. These conformers, as well as structures generated from many other different charge site assignments,[45] have calculated Ω_{asp} values that are consistent with the range of experimental values (Figure 2). Some $[Ala_n+2H]^{2+}$ charge site assignments result in extensive helical regions; however, these structures are higher in energy and calculated asphericities are larger than the experimental values. Although we cannot rule out the presence of specific regions of small helices in $[Ala_n+2H]^{2+}$ peptides, no strong evidence for this is found; it appears that any structured regions are randomly distributed in the $[Ala_n+2H]^{2+}$ family as observed previously for the $[Ala_n+H]^+$ globules.[20,21] We also note that the mobility data (Figure 1) for the +2 ions show peaks having full widths at half-maximum (fwhm) that are factors of 3 to 4 times broader than expected for transport of a single conformer type[46]—an indication that many unresolved states are present.

$[Ala_n+3H]^{3+}$: Evidence for Extended Helical and Hinged Helix-Coil Motifs. Simulations of many charge site assignments for $[Ala_{24}+3H]^{3+}$, $[Ala_{30}+3H]^{3+}$, $[Ala_{32}+3H]^{3+}$, $[Ala_{36}+3H]^{3+}$, and $[Ala_{40}+3H]^{3+}$ reveal structures that are much more specific than the globular structures found in simulations of $[Ala_n+H]^+$ and $[Ala_n+2H]^{2+}$. In particular, two types of structural motifs routinely emerge as the lowest energy structure for a given charge site assignment: an extended helical conformation and a hinged helix-coil structure. Figures 4 and 5 show typical conformers obtained from simulations of eight charge assignments of $[Ala_{36}+3H]^{3+}$. The average calculated asphericity of 0.416 ± 0.016 for the extended helices shown in Figure 4 is in good agreement with the 0.404 experimental value for the low mobility peak. These helices are comprised of ~90% $i \rightarrow i +$ 4 hydrogen bonding. There are slight disruptions (usually $i \rightarrow i + 3$ turns) near the positions of the charge sites. Similarly, an average value of $\Omega_{asp} = 0.299 \pm 0.010$ for the hinged helix-coil motifs in Figure 5 is in agreement with $\Omega_{asp}(expt) = 0.297$ for the high-mobility peak. Superimposed on the data in Figure 2 are calculated asphericities for the model extended helices and helix-coils found in simulations for a range of charge site

(45) For $[Ala_n+2H]^{2+}$ peptides, model structures were constructed by protonating the amino terminus and assigning the second charge to each of the backbone −NH groups along the chain.

(46) Mason, E. A.; McDaniel, E. W. *Transport Properties of Ions in Gases*; Wiley: New York, 1988.

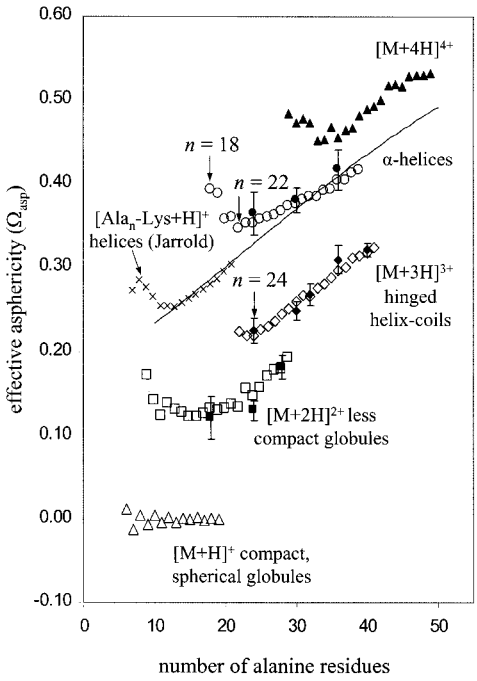

Figure 2. Effective asphericities derived from experimental data for $[Ala_n+H]^+$ (open triangles), $[Ala_n+2H]^{2+}$ (open squares), $[Ala_n+3H]^{3+}$ (n = 24−41, open diamonds; n = 18−39, open circles), and $[Ala_n+4H]^{4+}$ (filled triangles) ions. Calculated asphericities are shown for model structures obtained from molecular dynamics simulations for $[Ala_n+2H]^{2+}$ globules (solid squares; n = 18, 24 and 28), $[Ala_n+3H]^{3+}$ hinged helix-coil (solid diamonds; n = 24, 30, 32, 36, and 40), and helical conformers (solid circles; n = 24, 30, and 36). Uncertainties correspond to one standard deviation of the cross-section calculations for the range of stable folded states found from molecular modeling. Also shown are asphericities for $[Ala_n-Lys+H]^+$ ions containing 5 to 19 Ala residues (denoted as ×), derived from relative cross sections reported previously by Hudgins and co-workers (ref 22), which have been normalized to account for differences in mass associated with the Lys residue. The solid line corresponds to calculated values for α-helical Ala_n polymers ($\phi = -57°$, $\psi = -47°$) containing 10 to 50 residues.

assignments for the $[Ala_{24}+3H]^{3+}$, $[Ala_{30}+3H]^{3+}$, $[Ala_{32}+3H]^{3+}$, $[Ala_{36}+3H]^{3+}$, and $[Ala_{40}+3H]^{3+}$ ions. The comparison shows that these two types of structures agree with experiment for a wide range of polyalanine sizes.

The good initial agreement of the simulations and experiment for many charge site assignments encouraged us to conduct an extensive investigation of how charge site assignment influences conformation.[47] We have focused on the $[Ala_{36}+3H]^{3+}$ system. For some charge site assignments (often having 2 or more protons in close proximity), the lowest energy structures found were much higher in energy (>50 kcal·mol^{-1}) than typical calculated energies for structures that are clearly extended helices or folded hinged helix-coil motifs. Often these structures can be ruled out due to the poor agreement of calculated asphericities with experiment. Examples of four high-energy states (chosen randomly for several charge site assignments) that do not agree with experiment are shown in Figure 6.

One factor that appears to distinguish whether extended or folded states are favored in simulations is the net position of charge along the polypeptide chain. Simulations of $[Ala_{36}+3H]^{3+}$ and other polymer sizes having the net charge distributed on the C-terminal half of the peptide [i.e., $(\sum i)/3 > n/2$, where i corresponds to each charge site position and n is the total number of alanine residues in the peptide] yield primarily elongated helices. From the experimental data in Figure 2 it appears that the relatively large coulomb repulsion along shorter chains (i.e., the $[Ala_{18}+3H]^{3+}$ to $[Ala_{21}+3H]^{3+}$ ions) lengthens the peptide. Peptides with 22 or more residues appear to be capable of stabilizing a majority of $i \rightarrow i + 4$ hydrogen bonds. From the simulations, it appears that, unlike the +1 and +2 families, the +3 family can stabilize helices because the net charge can shift to the C-terminal side of the peptide, even if a proton is retained on the N-terminus. We also note that although the amine terminus is expected to be the most basic site in small alanine polypeptides,[48−50] this may not be the case for larger systems and it is possible that all three protons are positioned on the polypeptide backbone. In large polyalanine peptides, the presence of a large macrodipole associated with the helix may favor protonation along the polypeptide chain. This shift can be thought of as being similar to the shifts in solution pK_a values for acidic residues that are located in regions of helix relative to those found in regions with less long-range structural order.[51] We are currently exploring this idea in more detail for the +3 and +4 peptides.[52]

Shifting the charge distribution to the N-terminal side of the chain [i.e., $(\sum i)/3 < n/2$] yields structures that are characterized by a stretched coil region along the N-terminal side and a C-terminal helix stabilized by interactions with the charged sites. The coil portions of these structures often appear to be largely random, except that the charged residues associate with and stabilize regions of helix along the C-terminal side of the chain. Much of the $i \rightarrow i + 4$ hydrogen bonding along the C-terminal side is conserved; only the last few C-terminal hydrogen bonding interactions and those associated with the region near the middle of the peptide (at the hinge) vary substantially. This conformer type has calculated Ω_{asp} values (Figure 2) that are in good agreement with experimental values over the range of observed high-mobility $[Ala_n+3H]^{3+}$ peaks.

Do Extended and Folded States Exist as Zwitterions? Recently, the possibility that peptide ions form zwitterionic structures has received considerable attention.[4b,53−56] Williams and co-workers have presented evidence that singly protonated bradykinin exists in a salt-bridged configuration.[53] To explore this type of behavior in the polyalanine system, we have carried out molecular modeling studies of several zwitterionic configu-

(47) We have also performed simulations initiated from non-α-helical structures (i.e. extended or random globules). These typically yielded highly nonspecific conformations with higher energies than the helical or hinged helix-coil states found from helical precursors. The inability to observe the lower energy helical or folded states from nonhelical precursors suggests that much more extensive simulations (which are beyond the scope of this work) would be required to find the lower energy conformer types. In a number of simulations, conformers obtained from 3_{10}-helical starting structures with the net charge distributed on the C-terminal half of the polypeptide chain collapsed to structures having a substantial fraction of $i \rightarrow i + 4$ hydrogen bonds (α-helices) having calculated energies that are only a few kilocalories per mole higher than extended helices obtained from α-helical starting structures.

(48) Wu, Z.; Fenselau, C. *J. Am. Soc. Mass Spectrom.* **1992**, *3*, 863. Cheng, X.; Wu, Z.; Fenselau, C. *J. Am. Chem. Soc.* **1993**, *115*, 4844.
(49) Wu, J.; Lebrilla, C. B. *J. Am. Chem. Soc.* **1993**, *115*, 3270. Wu, J.; Lebrilla, C. B. *J. Am. Soc. Mass Spectrom.* **1995**, *6*, 91.
(50) Zhang, K.; Zimmerman, D. M.; Chung-Phillips, A.; Cassady, C. J. *J. Am. Chem. Soc.* **1993**, *115*, 10812.
(51) Joshi, H. V.; Meier, M. S. *J. Am. Chem. Soc.* **1996**, *118*, 12038−12044.
(52) Counterman, A. E.; Clemmer, D. E. Work in progress.
(53) Schnier, P. D.; Price, W. D.; Jockusch, R. A.; Williams, E. R. *J. Am. Chem. Soc.* **1996**, *118*, 7178.
(54) Wyttenbach, T.; Bushnell, J. E.; Bowers, M. T. *J. Am. Chem. Soc.* **1998**, *120*, 5098.
(55) Lee, S. W.; Kim, H. S.; Beauchamp, J. L. *J. Am. Chem. Soc.* **1998**, *120*, 3188.
(56) Freitas, M. A.; Marshall, A. G. *Int. J. Mass Spectrom.* **1999**, *183*, 221.

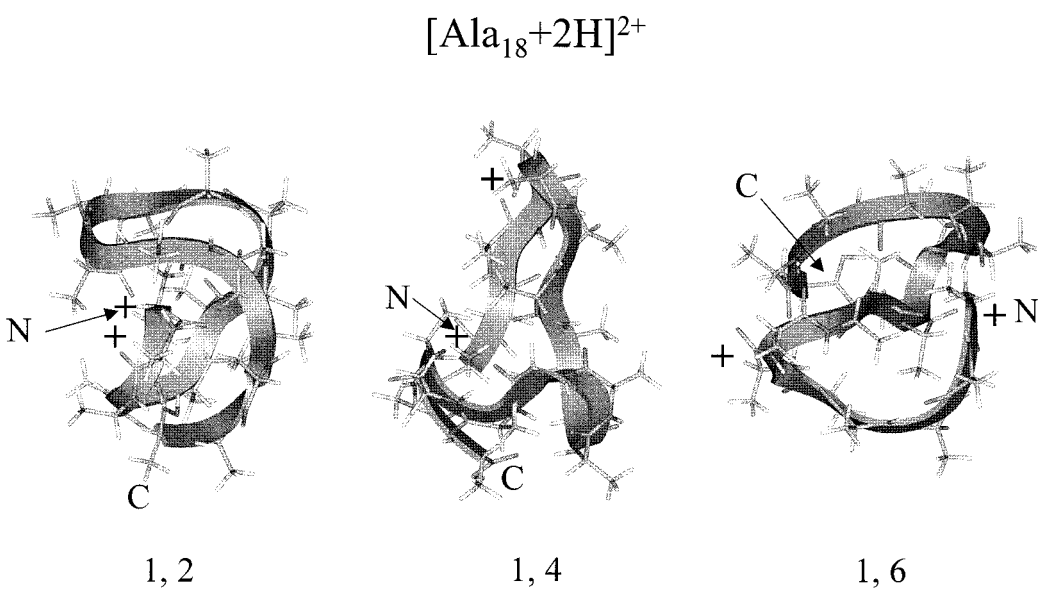

Figure 3. Three typical conformers found from 300 K molecular dynamics on initially α-helical structures for the 1, 2; 1, 4; and 1, 6 charge configurations of $[Ala_{18}+2H]^{2+}$ are shown. The N- and C-termini are labeled "N" and "C", respectively, and charge site positions are represented with "+" symbols. The globular structures that are found for these charge site assignments have calculated asphericities of 0.108, 0.125, and 0.109 that agree with the 0.132 experimental value. Charge solvation interactions are apparent; however, regions of helical turns appear to occur in what is largely a random fashion.

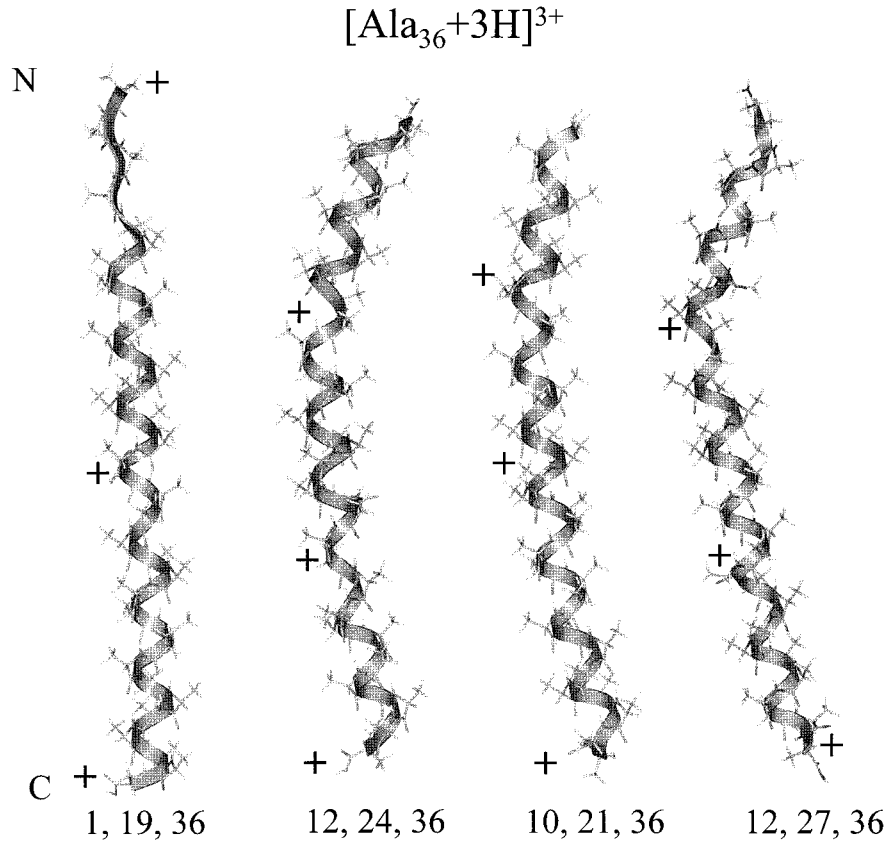

Figure 4. Typical conformers resulting from 300 K molecular dynamics simulations of the $[Ala_{36}+3H]^{3+}$ i = 1, 19, 36 (calculated Ω_{asp} and total energy of 0.423 and −119.6 kcal·mol^{-1}, respectively); 12, 24, 36 (0.416 and −162.0 kcal·mol^{-1}); 10, 21, 36 (0.408 and −161.1 kcal·mol^{-1}); and 11, 27, 36 (0.418 and −162.5 kcal·mol^{-1}) charge site assignments initiated from completely α-helical structures. Energies for these conformers are the lowest of those observed in each simulation, and calculated Ω_{asp} values are in agreement with the experimental value of 0.404. The N- and C-termini are labeled "N" and "C", respectively, and charge site positions are represented with "+" symbols.

rations of the Ala_{32} and Ala_{34} polymers. In these studies, the C-terminus is deprotonated and an additional proton is added to the N-terminal amine (or some other position along the polypeptide chain) such that the total charge is +3. Even with all of the protons positioned on the C-terminal side of the peptide, initial extended structures quickly collapse into more compact conformations. Overall, we found no evidence for extended conformations in any of our charge site assignments. Thus, we rule out the possibility that the extended state involves a zwitterionic structure.

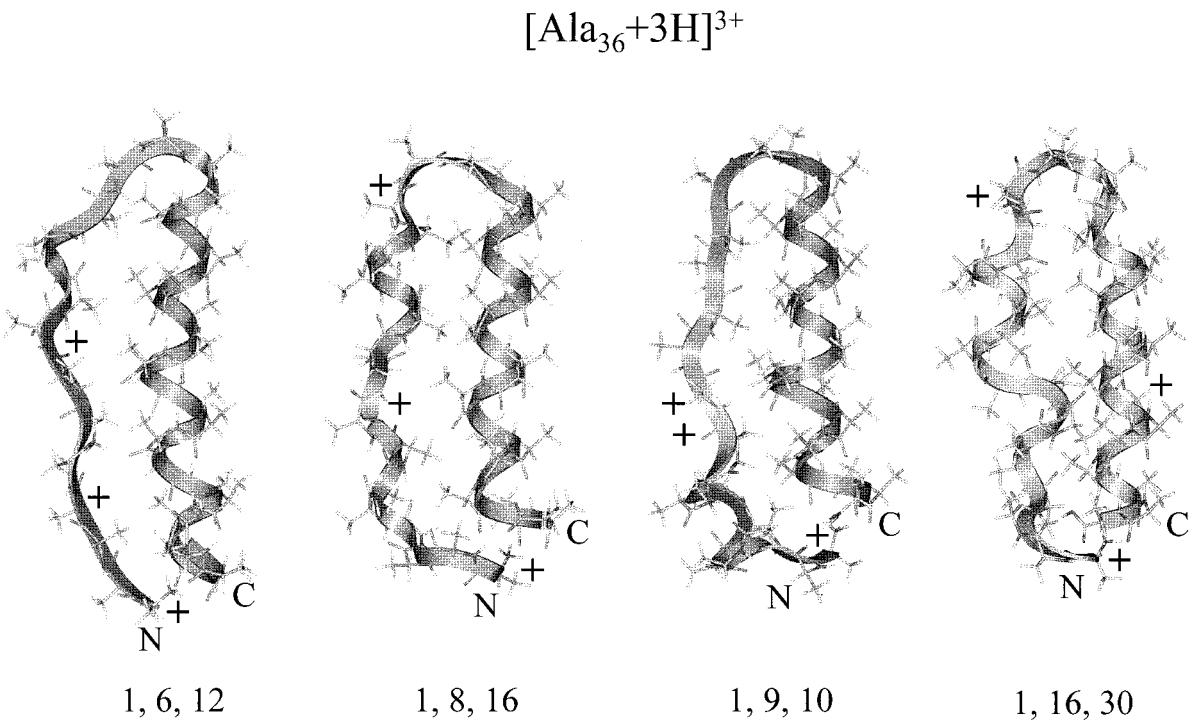

Figure 5. Typical conformers resulting from 300 K molecular dynamics simulations of $[Ala_{36}+3H]^{3+}$ $i = 1, 6, 12$ (calculated Ω_{asp} and total energy of 0.298 and −124.4 kcal·mol^{-1}, respectively); 1, 8, 16 (0.285 and −130.9 kcal·mol^{-1}); 1, 9, 10 (0.308 and −130.5 kcal·mol^{-1}); and 1, 16, 30 (0.289 and −142.8 kcal·mol^{-1}) charge site assignments initiated from completely α-helical structures. The hinged helix-coil conformer types that are shown for each of these charge site assignments are the lowest energy conformation found in each simulation, and calculated Ω_{asp} values are in agreement with the experimental value of 0.297. The N- and C-termini are labeled "N" and "C", respectively, and charge site positions are represented with "+" symbols.

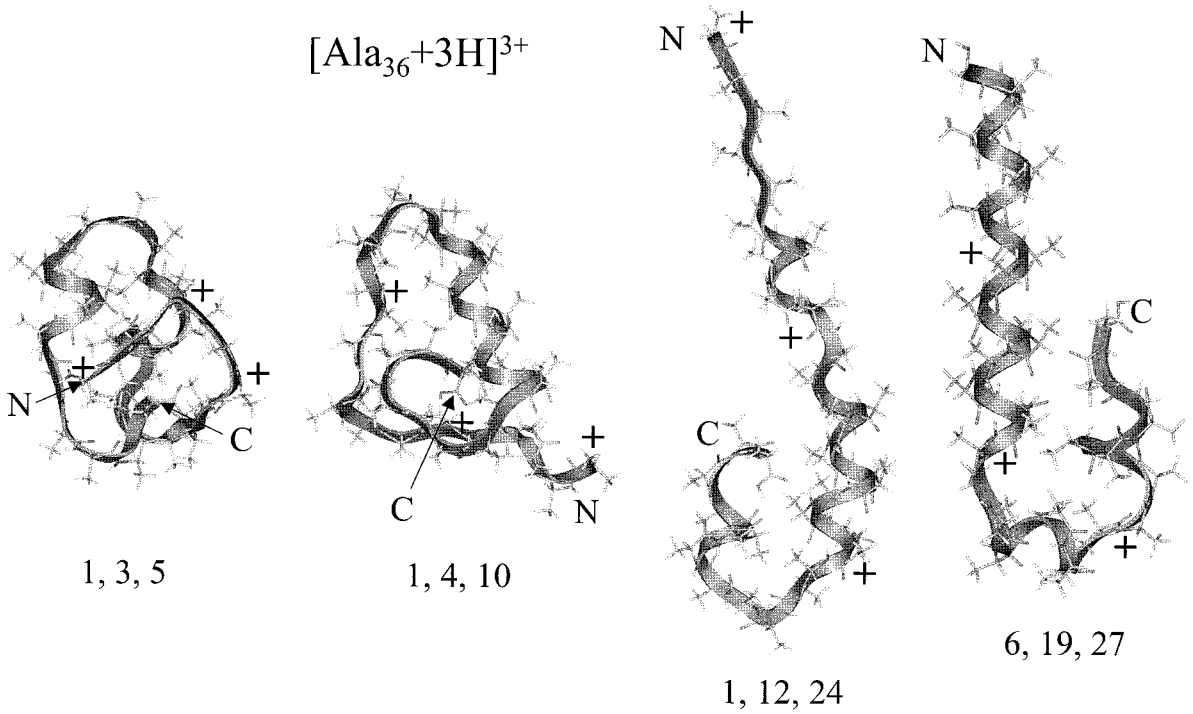

Figure 6. Lowest energy conformers obtained from 300 K molecular dynamics simulations of $[Ala_{36}+3H]^{3+}$ when charges are assigned to the 1, 3, 5 (calculated Ω_{asp} and total energy of 0.191 and −85.3 kcal·mol^{-1}, respectively); 1, 4, 10 (0.275 and −82.7 kcal·mol^{-1}); 1, 12, 24 (0.382 and −71.5 kcal·mol^{-1}); and 6, 19, 27 (0.370 and −96.4 kcal·mol^{-1}) positions. These conformers are typical of many other low-energy structures that were also found. All other aspects of the molecular dynamics simulations were identical with those used in Figure 4. Note that none of the calculated asphericities for the structures that are shown agrees with the experimental values of 0.297 and 0.404. The N- and C-termini are labeled "N" and "C", respectively, and charge site positions are represented with "+" symbols.

When the net charge is located on the N-terminal side of the peptide, the lowest energy zwitterionic structures that we found have globular (largely random) structures; the calculated asphericities for these states are substantially smaller than the experimental values measured for the higher mobility $[Ala_{32}+3H]^{3+}$ and $[Ala_{34}+3H]^{3+}$ ions. We note that if we

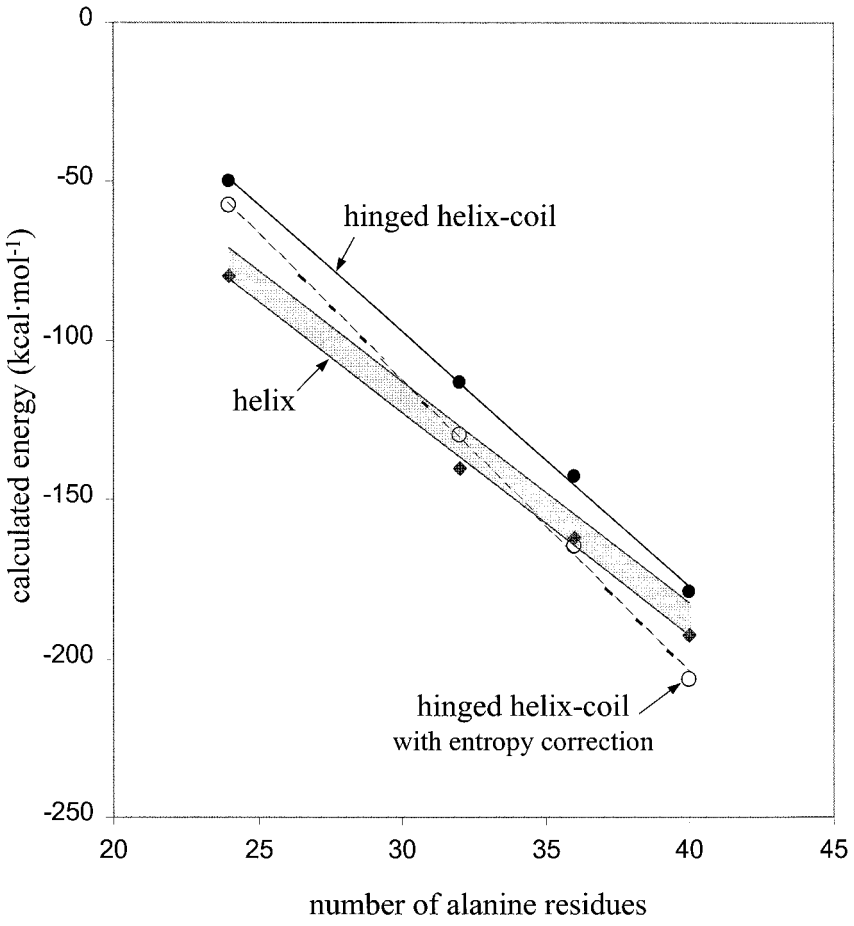

Figure 7. Lowest calculated energies from 300 K molecular dynamics simulations resulting in helical (solid diamonds) and hinged helix-coil states (solid circles) for $[Ala_n+3H]^{3+}$ (n = 24, 32, 36, 40). The open circles show calculated energies for the hinged helix-coil state that have been corrected by $T\Delta S$ associated with the coil region (taken to be $n/2$ residues) according to values provided in ref 61. The solid and dashed lines are linear fits to the calculated energies, and are intended as visual guides. The shaded region corresponds to an uncertainty of ~10 kcal·mol^{-1} associated with configurations that are not protonated at the amino terminus.

rearrange charges on a hinged helix-coil state configuration (generated as described above) to create a zwitterion, it is possible to generate structures that have calculated asphericities that agree with the experimental values; these structures appear to be stable over the timescale of the simulation and the final structures are very similar to the starting hinged helix-coil precursors. Thus, it is possible that the hinged helix-coil state exists as a zwitterion; however, neither the molecular modeling results nor experimental results allow us to distinguish between the zwitterionic or triply protonated hinged helix-coil state.

Relative Energies of Extended Helix and Hinged Helix-Coils. Comparison of the relative energies of lowest energy structures found in different simulations provides additional insight into this system. Hinged helix-coil motifs are generally the lowest energy structures found for a given $(\sum i)/3 < n/2$ charge site assignment. These states are lower in energy than structures from charge site assignments that show calculated asphericities in poor agreement with experiment, but are higher in energy than most extended helices that are found in simulations of $(\sum i)/3 > n/2$ assignments. For example, the lowest energy folded conformer found for $[Ala_{36}+3H]^{3+}$ was a hinged helix-coil generated for the i = 1, 16, 30 charge assignment;[57] the −142.8 kcal·mol^{-1} calculated energy for this structure is still 19.7 kcal·mol^{-1} higher than the lowest energy helix (i = 11, 27, 36; −162.5 kcal·mol^{-1}). The observation that the hinged helix-coil conformer has a higher calculated energy than the extended helical conformer seems to be inconsistent with the experimental observation that the hinged helix-coil state dominates the mobility distributions at larger polymer sizes.[58] One possible explanation is that the hinged helix-coil state is kinetically trapped during the electrospray process. Substantial evidence indicates that the electrospray process is sufficiently gentle to preserve noncovalent structure from solution.[7b,28,59,60] We have varied the solution conditions used to produce $[Ala_n+zH]^{z+}$ ions and find no variations in the relative abundances of peaks associated with the elongated and folded

(57) It should be noted that molecular dynamics simulations of the $[Ala_{36} + 3H]^{3+}$ i = 1, 16, 30 charge assignment started from an α-helical structure do not sample low-energy folded structures; instead, they yield higher energy conformers similar to the 1, 12, 24 conformer shown in Figure 6. The low-energy hinged helix-coil state was found by varying charge site assignments on hinged helix-coil starting structures.

(58) Uncertainties associated with the calculated ESFF energies as well as limitations in our ability to sample all conformations may influence this comparison. We expect that the relative energies of different conformations (for different charge site assignments for a given size) are accurate to within several kilocalories per mole. However, the force fields used in these calculations are still being tested and developed. For example, studies of Ala_4 have shown that the relative (qualitative) energetics obtained with empirical force fields differ in some cases from those derived from more rigorous ab initio calculations; see, for example: Beachy, M. D.; Chasman, D.; Murphy, R. B.; Halgren, T. A.; Friesner, R. A. *J. Am. Chem. Soc.* **1997**, *119*, 5908.

(59) Covey, T. R.; Douglas, D. J. *J. Am. Soc. Mass Spectrom.* **1993**, *4*, 616. Hudgins, R. R.; Woenckhaus, J.; Jarrold, M. F. *Int. J. Mass Spectrom. Ion Processes* **1997**, *165/166*, 497. Shelimov, K. B.; Jarrold, M. F. *J. Am. Chem. Soc.* **1997**, *119*, 2987.

(60) Light-Wahl, K. J.; Springer, D. L.; Winger, B. E.; Edmonds, C. G.; Camp, D. G., II; Thrall, B. D.; Smith, R. D. *J. Am. Chem. Soc.* **1993**, *115*, 803. Klassen, J. S.; Schnier, P. D.; Williams, E. R. *J. Am. Soc. Mass Spectrom.* **1998**, *9*, 1117.

$[Ala_n+3H]^{3+}$ ions over a range of solvent compositions that would normally trap different protein states.

Another explanation for the apparent discrepancy is that the calculated energies do not include contributions to the free energy from entropy. Okamoto and Hansmann have used multicanonical algorithms to calculate $T\Delta S$ terms for the helix-to-coil transition in Ala_{10}, Ala_{15}, and Ala_{20} of -4.5 ± 2.0, -14.2 ± 2.1, and -27.6 ± 2.7 kcal·mol^{-1}, respectively.[61] Considering that ~50% of residues in the hinged helix-coil state are involved in the coil (i.e. the N-terminal half), these terms can be applied as a correction for calculated energies of hinged polymers containing 20, 30, and 40 residues, respectively. Figure 7 shows a plot of the lowest calculated energies for the helical conformers and hinged helix-coils as well as a curve that includes a correction for the relative $T\Delta S$ difference for the hinged helix-coil and extended helical states. The entropic correction predicts that the free energy of the hinged helix-coil drops below the extended helix for ions with ~31 to 35 residues, near the 32 residue transition observed experimentally.

Finally, we consider the entropic correction for globular or randomly folded conformations found in the molecular dynamics simulations. For globular conformations, we approximated the $T\Delta S$ correction using the values for random coils obtained from multicanonical calculations and estimated a correction of -55.2 kcal·mol^{-1} for Ala_{40} (i.e., twice the calculated value for Ala_{20}). Typical calculated energies for the most stable $[Ala_{36}+3H]^{3+}$ globules are approximately -85 kcal·mol^{-1} (for example, see Figure 6); inclusion of the entropic term (-51 kcal·mol^{-1}) yields a final energy of -136 kcal·mol^{-1}, which is substantially higher than the -164.6 kcal·mol^{-1} value for the hinged helix-coil state. Even with the entropy correction, globular states for all polymer sizes that we have modeled are less energetically favorable than the helical and hinged helix-coil states. Thus, while the $T\Delta S$ correction for the folded hinged helix-coil states helps to rationalize the origin of the change in population of the high-mobility and low-mobility ions as a function of size, the entropic term does not appear to be sufficient to favor a fully random globule.

Summary and Conclusions

Ion mobility measurements for polyalanine ions $[Ala_n+H]^+$ ($n = 5$ to 19), $[Ala_n+2H]^{2+}$ ($n = 9$ to 29), $[Ala_n+3H]^{3+}$ ($n = 18$ to 41), and $[Ala_n+4H]^{4+}$ ($n = 29$ to 49) have been reported. Two series of $[Ala_n+3H]^{3+}$ conformations are observed: a family of elongated structures, for $n = 18$ to 39; and a series of more compact conformations, for $n = 24$ to 41. These conformations do not interconvert over the 10 to 30 ms experimental timescale, and the compact state dominates for $n > 32$. Molecular dynamics simulations suggest that the low-mobility family of conformers corresponds to an extended helical state. The higher mobility family is more difficult to assign; however, evidence suggests that this state corresponds to a folded state, in which the N-terminal side of the polypeptide adopts a largely random configuration while the C-terminal side has substantial helical quality—a hinged helix-coil state.

While the extended helical structure of polyalanine may be anticipated from previous condensed-phase work,[62] folded polyalanine structures have not been reported previously. The location of net charge appears to be important in stabilizing these conformer types and we have investigated how the location of charges along the polymer influences structure in detail. If charges are assigned such that $(\sum i)/3 > n/2$, extended helices are stabilized; if $(\sum i)/3 < n/2$, the polypeptide folds. Model structures for many different charge site assignments of the folded state show that the N-terminal portion of the polypeptide chain (e.g., residues 1 to 19 in the $[Ala_{36}+3H]^{3+}$ conformers shown) are largely extended chains. Presumably helical regions along the N-terminal side of the initial model helix are initially disrupted by charge solvation interactions, as observed previously for the $[Ala_n+H]^+$ globules;[20,21] the relatively high coulomb repulsion along the N-terminal portion of the chain forces it to adopt a stretched configuration, and charged sites are effectively stabilized through interactions with the C-terminal helix. Much of the $i \rightarrow i + 4$ hydrogen bonding along the C-terminal side is conserved; only the last few C-terminal hydrogen bonding interactions and those associated with the region near the middle of the peptide (at the hinge) vary substantially. It would appear that while the N-terminal coil stabilizes the C-terminal helix by charge-capping near the C-terminus, the bulk of the coil may be highly flexible; thus, entropy also may help stabilize the hinged helix-coil. At this point, the calculated energies for these states are virtually identical. Studies of these conformations as a function of temperature will be useful for resolving which conformer is most stable.

The 24-residue onset of this folded motif is near the smallest 23-residue peptide sequence that has been designed to fold in solution without external stabilizing forces.[2] While extended helices in the gas phase are analogous in many ways to solution helices, the relationship of the folded state to structures in solution remains largely unknown. It is possible that a folded hinged helix-coil competes with elongated helices in both media.

Acknowledgment. The authors gratefully acknowledge financial support from the National Science Foundation (CHE-9625199) and the National Institutes of Health (grant no. 1R01GM55647-01) and thank the reviewers for many insightful comments and suggestions.

JA9940625

(61) Okamoto, Y.; Hansmann, U. H. E. *J. Phys. Chem.* **1995**, *99*, 11276−11287.

(62) Fasman, G. D., Ed. *Poly-α-aminoacids*; Dekker: New York (1967).